

Proceedings of the Second Annual LHCP
CMS CR-2014/203
June 12, 2022

Inclusive searches for SUSY at CMS

CHRIS LUCAS

*On behalf of the CMS Experiment,
School of Physics
University of Bristol, UK.*

ABSTRACT

Multiple searches for supersymmetry have been performed at the CMS experiment. Of these, inclusive searches aim to remain as sensitive as possible to the widest range of potential new physics scenarios. The results presented in this talk use the latest 19.5fb^{-1} of 8 TeV data from the 2012 LHC run. Interpretations are given within the context of Simplified Model Spectra for a variety of both hadronic and leptonic signatures.

PRESENTED AT

The Second Annual Conference
on Large Hadron Collider Physics
Columbia University, New York, U.S.A
June 2-7, 2014

1 Introduction

Of the many proposed beyond the Standard Model (SM) theories, Supersymmetry (SUSY) still remains one of the best theoretically motivated and studied. A low energy realisation of SUSY with TeV-scale third-generation squarks [1] is motivated by the cancellation of the quadratically divergent loop corrections to the mass of the recently discovered Higgs boson [2, 3] in the SM without the need for significant fine tuning. For R-parity conserving SUSY [4], supersymmetric particles (sparticles) such as squarks and gluinos are produced in pairs and decay to the lightest, stable supersymmetric particle (LSP). The LSP is generally assumed to be weakly interacting and massive, hence a typical signature is a final state of multijets accompanied by significant missing transverse energy, \cancel{E}_T . Such a weakly interacting massive particle (WIMP) is considered to be a prime candidate for Dark Matter (DM).

Traditionally searches have interpreted results in terms of complete phenomenological models such as the Constrained Minimally Supersymmetric extension to the Standard Model (CMSSM)[5]. More recently however, analyses have moved from model-specific to signature-specific interpretations. Simple models are constructed which contain pair-produced sparticles which each decay with a 100% branching fraction to a given final state. By varying the sparticle masses, model scans and interpretations are produced which can be applied to a wide range of phenomenological models. Such models are known as Simplified Model Spectra (SMS) and will be the focus of the interpretations in the presented results.

CMS SUSY searches cover an expansive amount of SUSY decay phase space through the multiple, complimentary search regions and methodologies used. Perhaps the most wide-reaching are so-called ‘inclusive searches’ which aim to remain as generic as possible.

2 Analyses

In these proceedings multiple complimentary searches using the CMS detector [6] are detailed. Both hadronic and leptonic analyses are covered, with results and interpretations given in terms of a variety of different Simplified Model Spectra (SMS) models [7]. All of the searches detailed use the full CMS 2012 dataset consisting of 19.5fb^{-1} of data at $\sqrt{s} = 8\text{TeV}$, applying the latest CMS recommended reconstruction and ID criteria. Despite the different search techniques employed, each analysis has the common technique of utilising the large amounts of missing transverse energy (\cancel{E}_T) due to sparticle decays and the subsequent, non-interacting LSP.

Common kinematic variables used in the following analyses include the scalar sum of hadronic event activity, H_T , the vectorial sum of hadronic event activity, \cancel{H}_T and the previously mentioned vectorial sum of the transverse energies of all particles, \cancel{E}_T .

2.1 Multijet + \cancel{E}_T

A search for SUSY is performed in the all-hadronic channel, searching for large jet multiplicities and significant \cancel{E}_T , while vetoing any leptonic activity in the event [8]. This particular analysis remains inclusive by making no specific requirement on the number of b-tagged jets in the final state. The dominant backgrounds for such a hadronic analysis can be divided into sources of genuine and fake \cancel{E}_T , each of which will be described in the following paragraphs.

Genuine sources of \cancel{E}_T involve a decay of some particle to a final state containing at least one neutrino. The largest of these is from Z boson production, where the Z decays to a neutrino pair, with associated jet production. Similarly, decays of a W boson, whether directly produced or via top quark decay, produce a lepton and a neutrino, and are therefore able to enter the hadronic signal region of such an analysis when the lepton is either mis-identified or missed entirely. The background contribution from $Z(\nu\bar{\nu})$ +jets is estimated using a photon-enriched data control sample, relying on the kinematic similarity between Z and γ bosons at high- p_T . In order to mimic the \cancel{E}_T from the neutrinos in the Z-decay, the γ is not included in the calculation of discriminating event variables such as H_T and \cancel{H}_T . The ratio of the two production cross-sections ($R_{Z/\gamma}$) is measured in both simulation and data, before calculating a prediction which can be extrapolated into the signal region. Similar data-driven techniques are applied to estimate lost-lepton contributions.

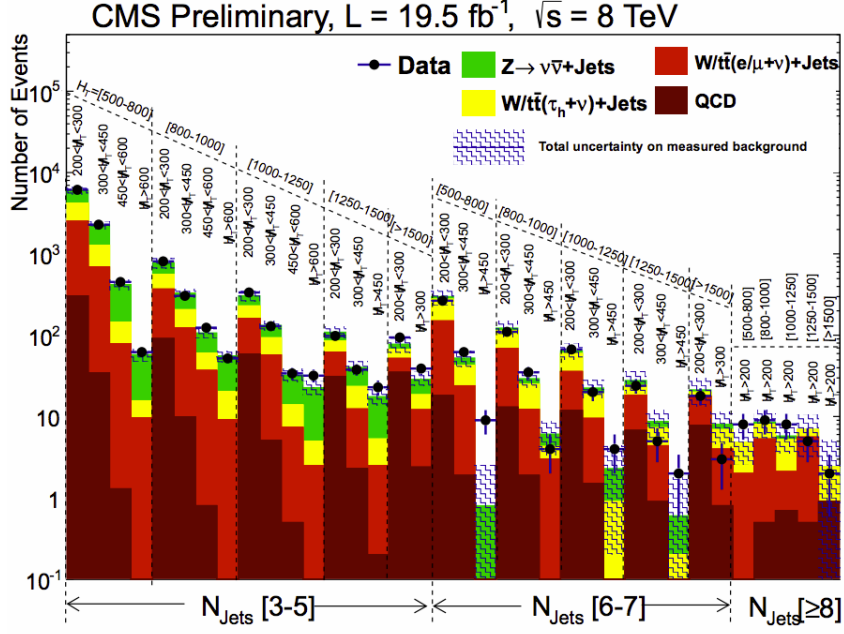


Figure 1: Data observations compared with background predictions for the Multijet + \cancel{E}_T analysis, split into bins of n_{jet} , H_T and \cancel{E}_T .

The main source of fake \cancel{E}_T comes from QCD multijet events, where jet mis-measurements can lead to significant amounts of \cancel{E}_T coupled with large numbers of jets. This background contribution is estimated using a rebalance and smearing technique on the event's jets [8], performed in kinematic sidebands to the signal region.

The analysis categorises events based on the event-variables H_T , \cancel{E}_T and the jet multiplicity, with results shown in this binning in Figure 1. No significant excess over the SM background predictions is observed in data and so limits are set in models of squark and gluino pair-production, shown in Figure 2.

The limit for light squark pair-production shown in Figure 2b has two exclusion curves. The stronger

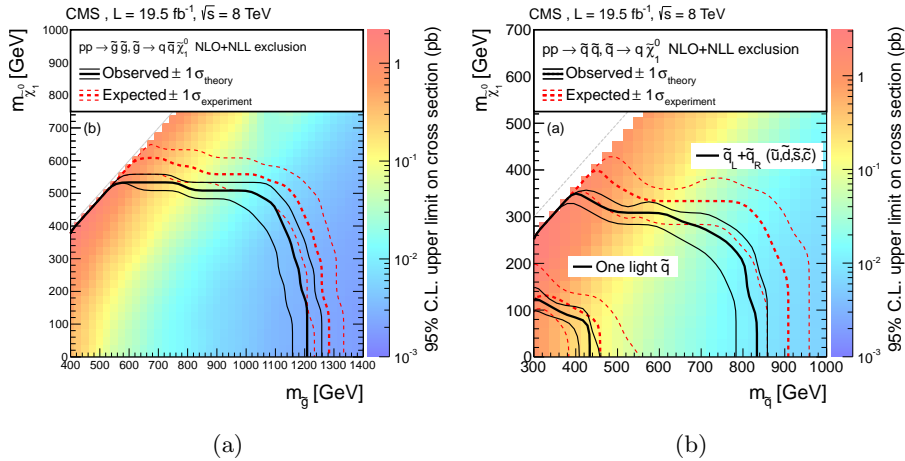


Figure 2: Multijet+ \cancel{E}_T results interpreted in simplified models of (2a) gluino pair-production, decaying via $\tilde{g} \rightarrow q\bar{q}\tilde{\chi}_1^0$ and (2b) squark pair-production, decaying via $\tilde{q} \rightarrow q\tilde{\chi}_1^0$

of the two considers a model in which production of all 4 light-squark flavours and their two helicities are available and degenerate. However the weaker of the two represents a model in which this 8-fold degeneracy is removed, and only a single light squark (of an arbitrary flavour and helicity) is produced.

2.2 MT2 Hadronic

The analysis described in this section makes use of a novel kinematic variable, M_{T2} , defined in Equation 1 as a function of the LSP pair mass ($m_{\tilde{\chi}}$) [9].

$$M_{T2}(m_{\tilde{\chi}}) = \min_{\vec{p}_T^{(1)} + \vec{p}_T^{(2)} = \vec{p}_T^{miss}} \left[\max(M_T^{(1)}, M_T^{(2)}) \right] \quad (1)$$

The M_{T2} variable can be thought of as a supersymmetric transverse mass, where the masses of the two ‘invisible’ LSP’s ($m_{\tilde{\chi}(1)}$ and $m_{\tilde{\chi}(2)}$) are determined from an events kinematic observables. The variable is used here as a discovery variable, where any excesses due to the presence of a supersymmetric decay would be evident in the high-mass tails of an M_{T2} distribution.

The analysis maintains sensitivity to a broad range of hadronic final states by binning in M_{T2} , H_T , n_{jet} and n_b . The M_{T2} analysis shares very similar backgrounds to the analysis described in the previous section due to the all-hadronic signal region. In order to estimate these background contributions to the signal region, data-driven techniques are also employed. As demonstrated above in section 2.1, one of the most significant backgrounds to an all-hadronic analysis is QCD multijet - a background which populates the low M_{T2} mass region. To reduce this background, a lower bound on the M_{T2} variable is chosen such that the QCD multijet contribution is considered negligible with respect to the total background prediction. This procedure is performed in each of the analysis categories, in dimensions of H_T , n_{jet} and n_b . Figure 3 shows the background composition in n_{jet} and n_b dimensions.

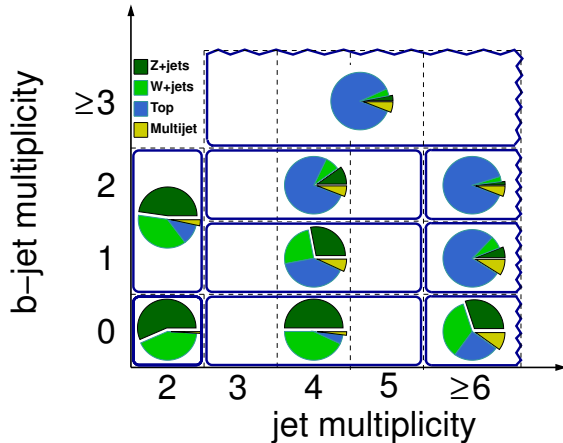


Figure 3: Background composition in categories of n_{jet} and n_b for an inclusive H_T and M_{T2} selection.

Results are shown in Figure 4 for the various H_T regions, subdivided into the multiple n_{jet} and n_b categories. As no significant excess in data is observed over the background prediction, limits are set in multiple models. Targeted interpretations are made using specific event categories with the strongest sensitivities to particular SMS models. Two examples are shown in Figure 5 where both squark and gluino production is considered, decaying to heavy quarks and subsequently large numbers of bottom quarks. Naturally high n_b categories are used, increasing signal acceptance while reducing the overall background. This targeted interpretation approach provides very strong limits for such high b-jet multiplicity models, and is also used for a variety of other signal models not shown here [9].

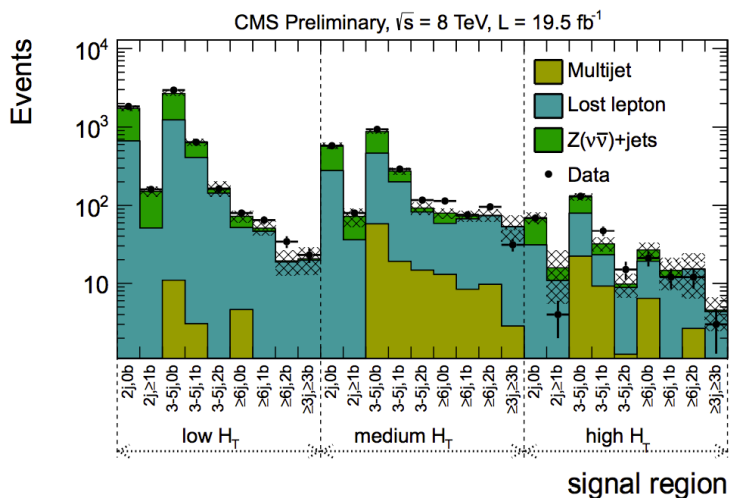


Figure 4: Data observations shown for each analysis category of the M_{T2} analysis, with the corresponding data-driven Standard Model background estimations.

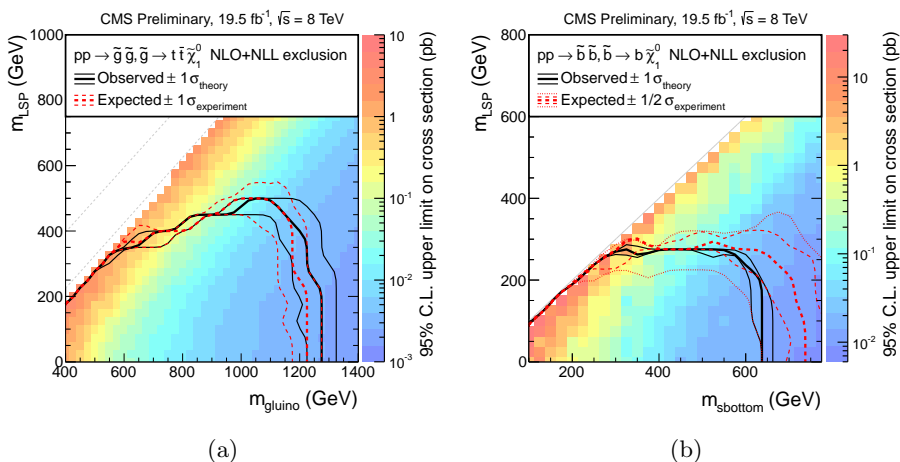


Figure 5: M_{T2} analysis results interpreted in simplified models of (5a) gluino pair-production, decaying via $\tilde{g} \rightarrow t\bar{t}\tilde{\chi}_1^0$ and (5b) sbottom pair-production, decaying via $\tilde{b} \rightarrow b\tilde{\chi}_1^0$.

2.3 Single lepton with btags

An inclusive search considers SUSY decays to a single lepton and multiple jets[10]. In such a leptonic final state, dominant standard model backgrounds come from semileptonic $t\bar{t}$ decays as well as W and Z boson leptonic decays, all estimated using data-driven techniques. The analysis consists of two complementary search strategies, one of which models the \cancel{E}_T distribution in exclusive bins of H_T , while the other relies on the measurement of the azimuthal angle between the mother-particle of the lepton, here assumed to be a standard model W, and it's daughter, $\Delta\phi(W, \ell)$. For the latter, under a standard model hypothesis, the kinematic constraints due to the mass of the W boson mother particle lead to an upper-bound on the value of $\Delta\phi(W, \ell)$, producing a sharp cutoff in the distribution. However, if the lepton originates from the decay of some supersymmetric particle, the mass of the mother particle can potentially be considerably higher, thereby increasing this upper-bound and populating the tails of a $\Delta\phi(W, \ell)$ distribution. A cut of $\Delta\phi(W, \ell) < 1.0$ is made on all events, greatly increasing the signal to background ratio in this signal region.

The analysis is binned in n_{jet} and n_b , as well as the scalar sum of transverse leptonic energy in the event,

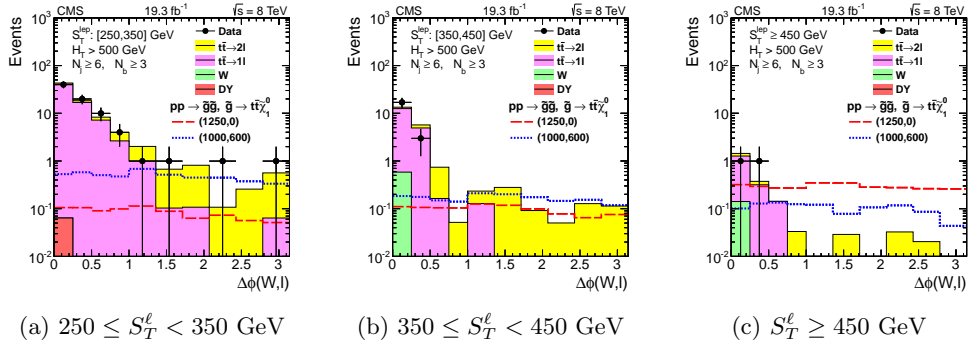


Figure 6: Results for the single lepton + b analysis, showing the $\Delta\phi(W, \ell)$ distributions for different S_T^ℓ bins in the $H_T > 500\text{GeV}$, $n_{jet} \geq 6$ and $n_b \geq 3$ category.

S_T^ℓ . Results for a given n_{jet} , and H_T category with the $\Delta\phi(W, \ell)$ method are shown in Figure 6.

No statistically significant excess is observed and so limits are placed in multiple models, two of which is shown in Figure 7. Strong exclusions in $m_{\tilde{g}}$, $m_{\tilde{t}_1}$ and $m_{\tilde{\chi}_0^0}$ are achieved due to the strong background discriminating power of the $\Delta\phi(W, \ell)$ method.

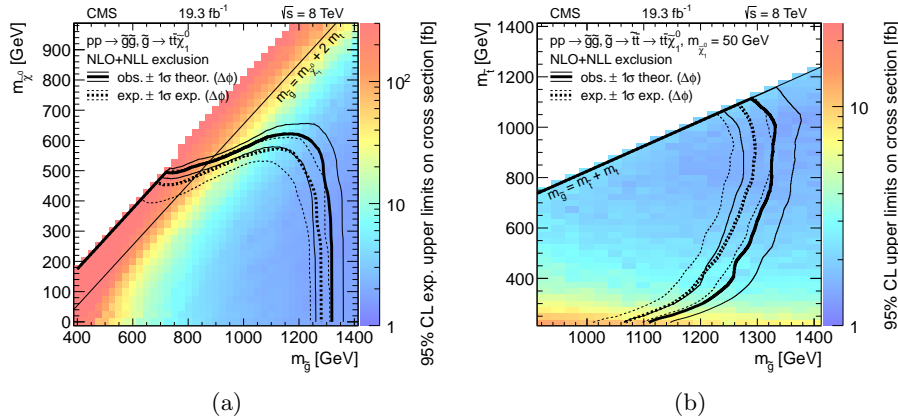


Figure 7: Limit from the single lepton + \cancel{E}_T search for the (7a) simplified model of gluino production, with the decay $\tilde{g} \rightarrow t\bar{t}\tilde{\chi}_1^0$, and (7b) gluino production with the decay $\tilde{g} \rightarrow t\bar{t} \rightarrow t\bar{t}\tilde{\chi}_1^0$.

2.4 Tri-lepton with btags

The final analysis considered here requires at least 3 leptons with associated b-tagged jets and \cancel{E}_T [11]. Although requiring such a high number of leptons reduces the SUSY production branch fraction, the effect is greatly offset by strongly suppressing any standard model backgrounds. Following these requirements, the only remaining backgrounds come from events with three prompt leptons, for example from WZ di-boson production, and a small contribution from rare standard model processes such as $t\bar{t} + V/H$, $t\bar{b} + Z$ and VVV (where V represents a vector boson). While the latter contribution is very small, the former is suppressed by the requirement of b-tagged jets.

The search is carried out in bins of H_T , \cancel{E}_T , n_{jet} and n_b , allowing the analysis to remain inclusive to a wide number of possible signal scenarios through targeted interpretation. By calculating the invariant mass of lepton pairs in the tri-leptonic system, two regions are formed as either ‘on’ or ‘off’ the Z-mass pole, with each region having different background compositions. Results for this binning schema are shown in Figure 8.

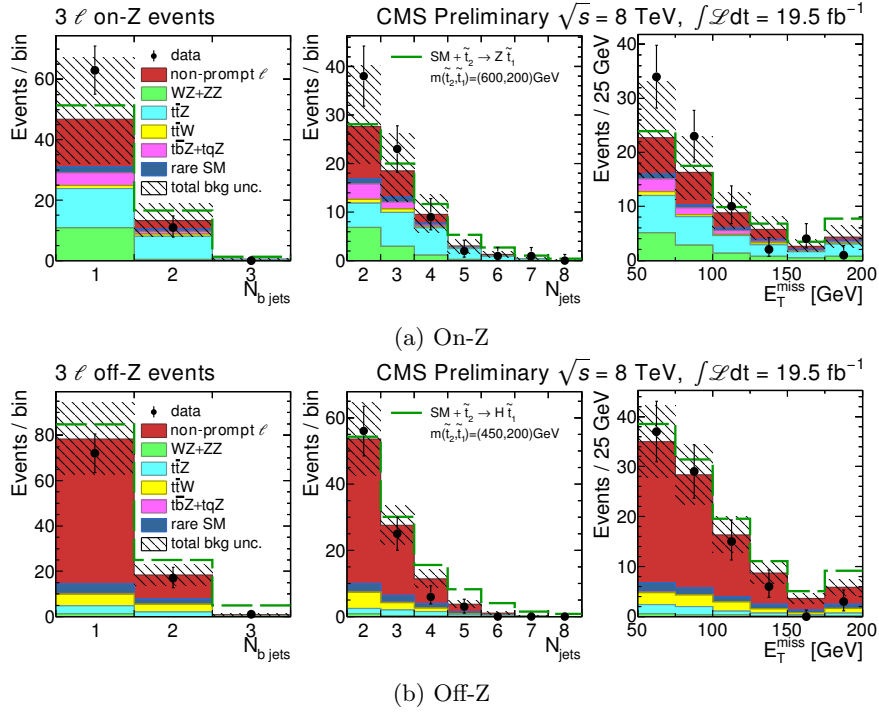


Figure 8: Results from the triplepton + b analysis, showing (8a) the on-Z mass and (8b) the off-Z mass regions.

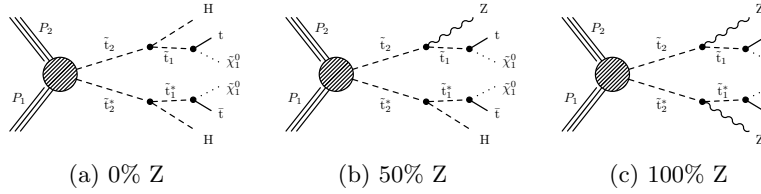


Figure 9: Model decays used for interpretation of the tri-lepton + b analysis.

As no significant excesses are observed, interpretations are made in a variety of models. Of these, one of particular interest is that of \tilde{t}_2 pair production, where the \tilde{t}_2 decays via the lighter \tilde{t}_1 with either $\tilde{t}_2 \rightarrow \tilde{t}_1 + Z$ or $\tilde{t}_2 \rightarrow \tilde{t}_1 + H$, followed by $\tilde{t}_1 \rightarrow t + \tilde{\chi}_1^0$, when $m_{\tilde{t}_1} - m_{\tilde{\chi}_1^0} \approx m_t$. This gives rise to the three scenarios shown in Figure 9, referred to by the relative branching fraction to Z-bosons in the decay. Figure 10a shows the limit from each Z-mass region for the 100% Z scenario (Figure 9c). As expected, the off-Z mass category drives the limit when the mass splitting between \tilde{t}_1 and \tilde{t}_2 becomes less than the mass of the Z, with the opposite being true for the on-Z category. Limits for all three decay scenarios are shown in Figure 10b, with the 100% Z limit being the strongest.

3 Conclusions

A selection of inclusive CMS SUSY searches were presented, using the full 19.7 fb^{-1} dataset collected in 2012. These included both leptonic and hadronic analyses, and are part of a much larger SUSY program which aims to cover the largest area of SUSY phase space possible with other inclusive and targeted searches. As no statistically significant signal has been observed in the current dataset, strong limits have been produced, for example gluino masses in excess of 1 TeV and stop masses up to 600 GeV dependent on the decay

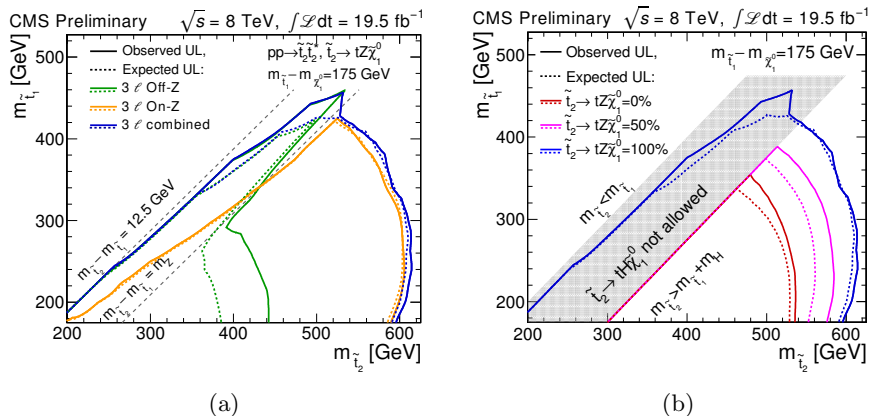


Figure 10: Limits from the trilepton + b analysis on the 100% scenario (10a), showing limits from the on and off Z-mass regions separately and combined, and for different admixtures of the \tilde{t}_2 decays via Z and H (10b).

mode. However, with the increase of \sqrt{s} in Run II, a significant gain in parton luminosity will be realised. As an example, the relative production cross section for a 1.5 TeV gluino will increase by a factor of 36 with respect to Run I. Despite the stringent limits presented here, significant amounts of SUSY phase space remain un-probed and so we look towards 2015 for a glimpse of supersymmetry at the LHC.

ACKNOWLEDGEMENTS

My sincere thanks go to the LHCP organisers for arranging a well-planned and fruitful conference, my CMS colleagues for running and delivering such high-quality data, in particular those that produced these competitive results, and my PhD supervisor for giving me the opportunity to attend this conference, eat too much of New York's food and a drink a large amount of it's beer.

References

- [1] R. Barbieri and D. Pappadopulo, JHEP **0910**, 061 (2009) [arXiv:0906.4546 [hep-ph]].
- [2] G. Aad *et al.* [The ATLAS Collaboration], Phys. Lett. B **716**, 1 (2012) [arXiv:1207.7214 [hep-ex]].
- [3] S. Chatrchyan *et al.* [The CMS Collaboration], Phys. Lett. B **716**, 30 (2012) [arXiv:1207.7235 [hep-ex]].
- [4] G. R. Farrar and P. Fayet, Phys. Lett. B **76**, 575 (1978).
- [5] S. Chatrchyan *et al.* [The CMS Collaboration], Phys. Rev. Lett. **107**, 221804 (2011) [arXiv:1109.2352 [hep-ex]].
- [6] S. Chatrchyan *et al.* [CMS Collaboration], JINST **3**, S08004 (2008).
- [7] J. Alwall, P. Schuster and N. Toro, Phys. Rev. D **79**, 075020 (2009) [arXiv:0810.3921 [hep-ph]].
- [8] S. Chatrchyan *et al.* [The CMS Collaboration], JHEP **1406**, 055 (2014) [arXiv:1402.4770 [hep-ex]].
- [9] S. Chatrchyan *et al.* [The CMS Collaboration], CMS-PAS-SUS-13-019.
- [10] S. Chatrchyan *et al.* [The CMS Collaboration], Phys. Lett. B **733**, 328 (2014) [arXiv:1311.4937 [hep-ex]].
- [11] V. Khachatryan *et al.* [The CMS Collaboration], Phys. Lett. B **736**, 371 (2014) [arXiv:1405.3886 [hep-ex]].